

# Chapter 5

## Self-Organized Criticality and Adaptation in Discrete Dynamical Networks

Thimo Rohlf and Stefan Bornholdt

**Abstract** It has been proposed that adaptation in complex systems is optimized at the critical boundary between ordered and disordered dynamical regimes. Here, we review models of evolving dynamical networks that lead to self-organization of network topology based on a local coupling between a dynamical order parameter and rewiring of network connectivity, with convergence towards criticality in the limit of large network size  $N$ . In particular, two adaptive schemes are discussed and compared in the context of Boolean Networks and Threshold Networks: (1) Active nodes loose links, frozen nodes acquire new links, (2) Nodes with correlated activity connect, de-correlated nodes disconnect. These simple local adaptive rules lead to co-evolution of network topology and -dynamics. Adaptive networks are strikingly different from random networks: They evolve inhomogeneous topologies and broad plateaus of homeostatic regulation, dynamical activity exhibits  $1/f$  noise and attractor periods obey a scale-free distribution. The proposed co-evolutionary mechanism of topological self-organization is robust against noise and does not depend on the details of dynamical transition rules. Using finite-size scaling, it is shown that networks converge to a self-organized critical state in the thermodynamic limit. Finally, we discuss open questions and directions for future research, and outline possible applications of these models to adaptive systems in diverse areas.

### 5.1 Introduction

Many complex systems in nature, society and economics are organized as networks of many interacting units that collectively process information or the flow of matter and energy through the system; examples are gene regulatory networks, neural networks, food webs in ecology, species relationships in biological evolution, economic interaction and the internet. From an abstract point of view, one can distinguish *network structure*, i.e. the (typically directed) graph that describes the wiring of interactions between the nodes the network is composed of, and *network dynamics*, refer-

---

T. Rohlf (✉)

Max-Planck-Institute for Mathematics in the Sciences, Inselstrasse 22, 04103 Leipzig, Germany  
e-mail: rohlf@mis.mpg.de

ring to certain state variables assigned to the nodes which can change in response to inputs or perturbations from other nodes. In the case of the genome, for example, dynamics of regulatory networks, as captured in changes of gene expression levels, results from repression and -activation of gene transcription controlled by regulatory inputs (transcription factors) from other genes [25].

A main characteristic of all these systems is that they evolve in time, under the continuous pressure of adaptation to highly dynamic environments. Since network topology and dynamics *on* the network are typically tightly interrelated, this implies a co-evolutionary loop between a time-varying network wiring and adaptive changes in the nodes' dynamics. For example, there is evidence from the analysis of gene regulatory networks that interactions between genes can change in response to diverse stimuli [58], leading to changes in network topology that can be far greater than what is expected from random mutation. In the case of nervous systems, it is evident that self-organization and adaptation processes have to continue throughout the lifetime of a network, since learning is a major function of such networks. In this context, a major conceptual challenge lies in the fact that, in order to properly function as information processing systems, adaptive networks have to be, on the one hand, highly robust against *random* (or dys-functional) perturbations of wiring and dynamics (noise) [5, 9, 90], and, on the other hand, stay responsive to essential cues (information) from the environment that can change in time. While robustness would clearly favor highly ordered dynamics that is basically insensitive to any perturbation, sensitivity and adaptive pressure tend to favor an ergodic sampling of the accessible state space. The latter comes with the risk of leading network evolution into regimes of chaotic dynamics with large parameter ranges where network dynamics is not easily controlled [63].

Two interesting and interrelated questions arise: First, is there a critical point, given by specific values of order parameters that characterize network topology and -dynamics, where adaptive dynamics with its delicate balance between robustness and flexibility is optimized? Second, can we find simple, very general principles of network self-organization from *local* co-evolutionary rules that couple network rewiring and -dynamics such that the network globally evolves to this point?

In the inanimate world, phase transitions from ordered to disordered dynamics at critical values of a system parameter are found in several classes of many particle systems, as for example in ferromagnets, where the system can maintain spontaneous magnetization below the Curie temperature, while above this critical point disorder induced by thermal fluctuations wins. Similar transitions from an organized to a disorganized state also have been observed in living systems, for example in enzyme kinetics [64], growth of bacterial populations [66] and brain activity [43]. Most biological networks are different in many regards from the many particle systems as considered in standard statistical mechanics. In particular, interactions between units are typically asymmetric and directed, such that a Hamiltonian (energy function) does not exist. Furthermore, to make global dynamical properties accessible despite the overall stunning degree of complexity found in these networks, a number of simplifying assumptions have to be made.

In this line, random Boolean networks (RBN) were proposed as simplified model of large gene regulatory networks [39, 88]. In these models, each gene receives a constant number  $K$  of regulatory inputs from other genes. Time is assumed to proceed in discrete steps. Each gene  $i$  is either “on” or “off”, corresponding to a binary state variable  $\sigma_i \in \{0, 1\}$ , which can change at time  $t$  according to a (fixed) Boolean function of its inputs at time  $t - 1$  (a more formal definition will be given in Sect. 5.2.2). RBNs can easily be generalized to a variable number of connections per node, and “biased” update rules<sup>1</sup> Despite its simple deterministic update rule, this model exhibits rich dynamical behavior. In particular, RBNs exhibit an order-disorder phase transition when each unit has on average two inputs from other nodes<sup>2</sup> [29].

Combinatorial and statistical methods have provided quite detailed knowledge about properties of RBNs near criticality [3, 4, 11, 12, 16, 17, 23, 24, 30, 32, 35, 40–42, 44, 45, 55–57, 79, 83]. The second class of discrete dynamical networks that we will consider are Random Threshold Networks (RTN) with sparse asymmetric connections (for details, cf. Sect. 5.2.3). Networks of this kind were first studied as diluted, non-symmetric spin glasses [26] and diluted, asymmetric neural networks [28, 47]. For the study of topological questions in networks, a version with discrete connections  $c_{ij} = \pm 1$  is convenient and will be considered here. It is a subset of Boolean networks with similar dynamical properties. Random realizations of these networks exhibit complex non-Hamiltonian dynamics including transients and limit cycles [10, 49]. In particular, a phase transition is observed at a critical average connectivity  $K_c$  with lengths of transients and attractors (limit cycles) diverging exponentially with system size for an average connectivity larger than  $K_c$ . A theoretical analysis is limited by the non-Hamiltonian character of the asymmetric interactions, such that standard tools of statistical mechanics do not apply [28]. However, combinatorial as well as numerical methods provide a quite detailed picture about their dynamical properties and correspondence with Boolean Networks [10, 11, 27, 29, 30, 35, 48, 49, 57, 65, 75, 77, 79].

From the observation that complex dynamical behavior in these simple model systems is primarily found near criticality, Kauffman [39, 40] and other researchers [50, 91] postulated that evolution should drive living systems to this “edge of chaos”. Indeed, a number of parameters that are highly relevant for biological systems, as, for example, robustness [40] and basin entropy [46] of attractors (limit cycles), mutual information in the switching dynamics of nodes [55, 73] and information diversity in structure-dynamics relationships [68] are maximized near the order-disorder transition of RBNs, supporting the idea that this point provides unique properties for balancing the conflicting needs of robustness and adaptive flexibility. Today, experimental results provide strong support for the idea that many biological

---

<sup>1</sup> The bias is typically parameterized in terms of a stochastic control parameter  $p$ , which determines the probability that a particular input configuration generates the output “1”.

<sup>2</sup> This critical connectivity  $K_c = 2$  refers to the simplest case, when all Boolean functions have equal probability to occur. For the case of biased update rules, this generalizes to  $K_c = 1/(2p(1 - p))$ .

systems operate in a regime that shares relevant properties with criticality in random networks. Indications for critical behavior were found, for example, in gene expression dynamics of several organisms [67, 72, 82] and in neuronal networks in the brain [14, 52]. Since, in all these systems, there generally exists no central control that could continuously adjust system parameters to poise dynamics at the critical state, we are *forced* to postulate that there are simple, *local* adaptive mechanisms present that are capable of driving *global* dynamics to a state of *self-organized criticality*. Evolution towards self-organized criticality was established in a number of non-equilibrium systems [6], namely, avalanche models with extremal dynamics [8, 71], multi-agent models of financial markets [59], forest fires [60] and models of biological macroevolution [31]. Still, these approaches are limited in the sense that they consider a fixed or at least pre-structured topology.

Network models of *evolving* topology, in general, have been studied with respect to critical properties earlier in other areas, e.g., in models of macro-evolution [84]. Network evolution with a focus on gene regulation has been studied first for Boolean networks in [20] observing self-organization in network evolution, and for threshold networks in [21]. Combining the evolution of Boolean networks with game theoretical interactions is used for model networks in economics [70].

Christensen et al. [22] introduced a static network with evolving topology of undirected links that explicitly evolves towards a critical connectivity in the largest cluster of the network. In particular they observed for a neighborhood-oriented rewiring rule that the connectivity of the largest cluster evolves towards the critical  $K_c = 2$  of a marginally connected network. However, in this model the core characteristics of adaptive networks, a co-evolution between dynamics and topology [37], is hard to establish, since the evolution rule, here chosen according to the Bak-Sneppen model of self-organized criticality [7], does not provide a direct coupling between rewiring of connections and an order parameter of the dynamics *on* the networks.

Keeping the idea of local connectivity adaptations, a different line of research pursues models of adaptive co-evolutionary networks in the context of discrete dynamical networks, in particular based on RBNs and RTNs. The common principle in these models is the coupling of *local* rewiring events to approximate, local measurements of a dynamical order parameter. In the limit of large network sizes  $N$ , this principle leads to network evolution towards a *global* self-organized critical state. Bornholdt and Rohlf [19] introduced a topology-evolving rule based on the dynamical activity of nodes in RTNs: Active nodes, whose binary state changes in time, tend to lose links, while inactive (frozen) nodes, whose binary states are fixed, tend to gain new links. In a recent extension [76], also adaptive changes of the nodes' activation thresholds were considered. A very similar co-evolutionary rule was applied to RBNs by Liu and Bassler [53]; besides the case where only the rewired node is assigned a new Boolean function, they also consider "annealed" networks, where each node is assigned a new logical function in each evolutionary time step. Teuscher and Sanchez [87] showed that this adaptive principle can also be applied to turing neural networks. Self-organized critical neural networks with stochastic dynamics and a rewiring rule based on dynamical correlations between

nodes was studied by Bornholdt and Röhl [18], observing robust self-organization of both network topology and -dynamics. In the same context, Bertschinger et al. [15] studied a synaptic scaling rule leading to self-organized criticality in recurrent neural networks. A different adaptive scheme, based on an input-dependent disconnection rule and a minimal connectivity in RBNs, was studied by Luque et al. [54]. A perturbation analysis indicates the emergence of self-organized critical behavior.

The remainder of this chapter is organized as follows: in Sect. 5.2, the dynamics of RBNs and RTNs are defined and basic dynamical and statistical properties of these systems are summarized. In particular, central order parameters that are relevant for the definition of adaptive algorithms will be introduced. In Sect. 5.3, we will review different models of adaptive, discrete dynamical networks leading to evolution towards self-organized criticality that have been established in this context so far, with a focus on activity- and correlation-based rewiring rules. Finally, Sect. 5.4 contains a summary and conclusions.

## 5.2 Dynamics of Random Boolean Networks and Random Threshold Networks

In this section, we provide definitions for the two types of discrete dynamical networks under consideration, Random Boolean Networks and Random Threshold Networks. First, the underlying graph structure that connects dynamical units (automata) is defined, then dynamical update rules are provided. Further, basic dynamical properties of these systems are summarized.

### 5.2.1 Underlying Graph Structure

Concerning topology, discrete dynamical networks are described by *random directed graphs*  $G(N, Z, g)$ , where  $N$  is the number of nodes,  $Z$  the number of edges or links (arrows connecting nodes), and  $g$  a function that describes the statistical distribution of the links between nodes. Arrows pointing *at* a node are considered as *inputs*, arrows pointing *from* this node *to* another node as *outputs*. If, for example,  $Z$  links out of the  $2N^2$  possible are assigned at random such that the average connectivity  $\bar{K} := Z/N$  is fixed at a predefined value and  $Z \ll 2N^2$  (sparse network), the resulting statistical distributions of the number  $k$  of inputs and outputs follow a Poissonian [34]:

$$P(k) = \frac{\bar{K}^k}{k!} \exp(-\bar{K}). \quad (5.1)$$

A schematic example of interaction graph structure is shown in the left panel of Fig. 5.1.

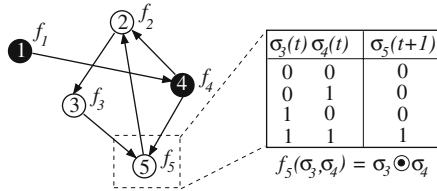


**Fig. 5.1** *Left panel:* example of an interaction graph structure for a RBN of size  $N = 5$  with average connectivity  $\bar{K} = 6/5$ ;  $f_i$  are individual Boolean functions assigned to each node  $i = 1, \dots, 5$ , *black circles* mark  $\sigma_i = 1$ , *white circles*  $\sigma_i = 0$ . *Right panel:* example of a Boolean update table assigned to a site (AND function of the site's inputs)

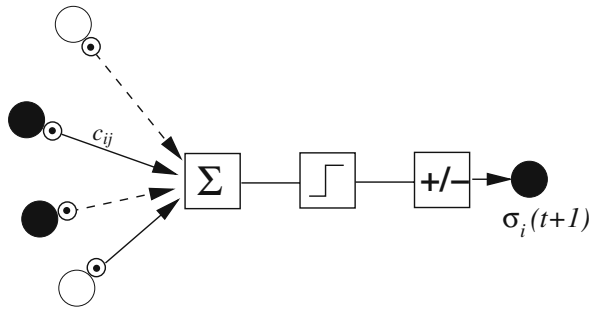


**Fig. 5.2** Schematic sketch of a threshold dynamical unit: input states (*circles on the left, black circles* correspond to a state  $\sigma_j = +1$ , *white circles* to  $\sigma_j = -1$ ) are multiplied ( $\odot$ ) with interaction weights  $c_{ij}$  (*lined arrows:*  $c_{ij} = +1$ , *dashed arrows:*  $c_{ij} = -1$ ); these values are summed ( $\Sigma$ ) and added to a threshold. Finally, the output  $\sigma_i(t + 1)$  is determined by the sign ( $+/-$ ) of the resulting signal

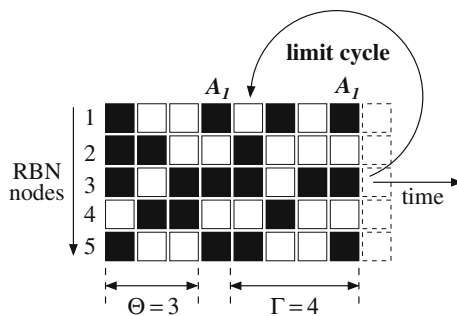


**Fig. 5.3** Example of a dynamical trajectory for a  $N = 5$  Boolean network, time is running from *left to right*, network nodes are labeled from *top to bottom*. *Black squares* correspond to  $\sigma_i = 1$ , *white squares* to  $\sigma_i = 0$ . After a transient of  $\Theta = 3$  system states  $\Sigma$  the first state  $A_1$  appears that repeats itself after  $\Gamma = 4$  time steps, defining a periodic attractor (limit cycle) with period 4

### 5.2.2 Random Boolean Networks

A Random Boolean Network (RBN) is a discrete dynamical system composed of  $N$  automata. Each automaton is a Boolean variable with two possible states:  $\{0, 1\}$ , and the dynamics is such that

$$\mathbf{F} : \{0, 1\}^N \mapsto \{0, 1\}^N, \quad (5.2)$$

where  $\mathbf{F} = (f_1, \dots, f_i, \dots, f_N)$ , and each  $f_i$  is represented by a look-up table of  $K_i$  inputs randomly chosen from the set of  $N$  automata. Initially,  $K_i$  neighbors and a look-up table are assigned to each automaton at random.

An automaton state  $\sigma_i(t) \in \{0, 1\}$  is updated using its corresponding Boolean function:

$$\sigma_i(t+1) = f_i(\sigma_{i_1}(t), \sigma_{i_2}(t), \dots, \sigma_{i_{K_i}}(t)). \quad (5.3)$$

We randomly initialize the states of the automata (initial condition of the RBN). The  $N$  automata are updated synchronously using their corresponding Boolean functions, leading to a new system state  $\Sigma := (\sigma_1, \dots, \sigma_N)$ :

$$\Sigma(t+1) = \mathbf{F}(\Sigma(t)). \quad (5.4)$$

The right panel of Fig. 5.1 provides an example of an individual update table assigned to a network site.

### 5.2.3 Random Threshold Networks

A Random Threshold Network (RTN) consists of  $N$  randomly interconnected binary sites (spins) with states  $\sigma_i = \pm 1$ . For each site  $i$ , its state at time  $t+1$  is a function of the inputs it receives from other spins at time  $t$ :

$$\sigma_i(t+1) = \text{sgn}(f_i(t)) \quad (5.5)$$

with

$$f_i(t) = \sum_{j=1}^N c_{ij} \sigma_j(t) + h. \quad (5.6)$$

The  $N$  network sites are updated synchronously. In the following discussion the threshold parameter  $h$  is set to zero. The interaction weights  $c_{ij}$  take discrete values  $c_{ij} = +1$  or  $-1$  with equal probability. If  $i$  does not receive signals from  $j$ , one has  $c_{ij} = 0$ .

## 5.2.4 Basic Dynamical Properties of RBNs and RTNs

Let us review a few aspects of the dynamics of Random Boolean Networks and Random Threshold Networks. In fact, they share most basic properties which is closely related to the fact that RTNs are a subset of RBNs.

### 5.2.4.1 Attractors and Transients

Update dynamics as defined in 5.2.2 and 5.2.3, given the binary state  $\sigma_i(t)$  of each node  $i$  at time  $t - 1$ , assigns a state vector  $\Sigma(t) = (\sigma_1(t), \dots, \sigma_N(t))$  to the network at each discrete time step  $t$ . The path that  $\Sigma(t)$  takes over time  $t$  is a dynamical trajectory in the phase space of the system. Since the dynamics is deterministic and the phase space of the system is finite for finite  $N$ , all dynamical trajectories eventually become periodic. When we start dynamics from a random initial state, e.g. with each  $\sigma_i(0)$ ,  $i = 1 \dots N$  set to 0 or 1 ( $-1$  or  $+1$  for RTN, respectively) independent from each other with equal probability  $p = 1/2$ , the trajectory will pass through  $\Theta$  transient states before it starts to repeat itself, forming a limit cycles given by

$$\Sigma(t) = \sigma(t + \Gamma). \quad (5.7)$$

The periodic part of the trajectory is the attractor of the dynamics, and the minimum  $\Gamma \geq 1$  that satisfies Eq. (5.7) is the *period* of the attractor.

### 5.2.4.2 Definition of Average Activity and Average Correlation

Let us now define two *local* measures that characterize the typical dynamical behavior of a network site, and the dynamical coordination of pairs of sites.

The *average activity*  $A(i)$  of a site  $i$  is defined as the average over all states  $\sigma_i(t)$  site  $i$  takes in dynamical network evolution between two distinct points of time  $T_1$  and  $T_2$ :

$$A(i) = \frac{1}{T_2 - T_1 + 1} \sum_{t=T_1}^{T_2} \sigma_i(t) \quad (5.8)$$

“Frozen” sites  $i$  which do not change their states between  $T_1$  and  $T_2$  obviously have  $|A(i)| = 1$  (or  $|A(i)| = 0$ , in the case of RBN), whereas sites that occasionally change their state have  $0 \leq |A(i)| < 1$ . The *average correlation*  $\text{Corr}(i, j)$  of a pair  $(i, j)$  of sites is defined as the average over the products  $\sigma_i(t)\sigma_j(t)$  in dynamical network evolution between two distinct points of time  $T_1$  and  $T_2$ :

$$\text{Corr}(i, j) = \frac{1}{T_2 - T_1 + 1} \sum_{t=T_1}^{T_2} \sigma_i(t)\sigma_j(t) \quad (5.9)$$



If the dynamical activity of two sites  $i$  and  $j$  in RTN is (anti-)correlated, i.e. if  $\sigma_i$  and  $\sigma_j$  always have either the same or the opposite sign, one has  $|\text{Corr}(i, j)| = 1$ .<sup>3</sup> If the relationship between the signs of  $\sigma_i$  and  $\sigma_j$  occasionally changes, one has  $0 \leq |\text{Corr}(i, j)| < 1$ .

### 5.2.4.3 Properties of $A(i)$ and $\text{Corr}(i, j)$ and Their Relation to Criticality

If we consider statistical ensembles of randomly generated networks with sparse wiring ( $\bar{K} \ll N$ ), both  $A(i)$  and  $\text{Corr}(i, j)$  of RBNs and RTNs exhibit a second order phase transition at a critical average connectivity  $K_c$  (averaged over the whole network ensemble). Below  $K_c$ , network nodes are typically frozen, above  $K_c$ , a finite fraction of nodes is active; this can be clearly appreciated from the behavior of the *frozen component*  $C(\bar{K})$ , defined as the fraction of nodes that do not change their state along the attractor. The average activity  $A(i)$  of a frozen site  $i$  thus obeys  $|A(i)| = 1$ . In the limit of large  $N$ ,  $C(K)$  undergoes a transition at  $K_c$  vanishing for larger  $K$ . With respect to the average activity of a node,  $C(K)$  equals the probability that a random site  $i$  in the network has  $|A(i)| = 1$ . Note that this is the quantity which is checked stochastically by the local rewiring rule that will be discussed in Sect. 5.3.1.2. The frozen component  $C(K, N)$  is shown for random networks of two different system sizes  $N$  in Fig. 5.4. One finds that  $C(K, N)$  can be approximated by

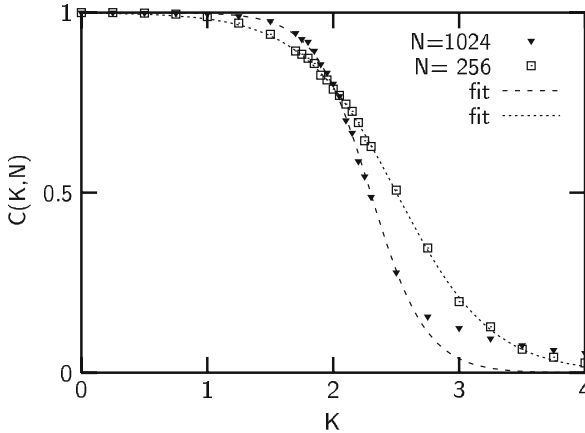


**Fig. 5.4** The frozen component  $C(K, N)$  of random threshold networks, as a function of the networks' average connectivities  $K$ . For both system sizes shown here ( $N = 256$  and  $N = 1,024$ ) the data were measured along the dynamical attractor reached by the system, averaged over 1,000 random topologies for each value of  $K$ . One observes a transition around a value  $K = K_0$  approaching  $K_c = 2$  for large  $N$ . A sigmoid function fit is also shown. To avoid trapping in exponential divergence of attractor periods for  $K > 2$ , the simulations have been limited to  $T_{max} = 10,000$ . The mismatch of data and fit for  $N = 1,024$ ,  $K \geq 2.75$  is due to this numerical limitation

<sup>3</sup> In RBN, correlated pairs have  $|\text{Corr}(i, j)| = 1$  and anti-correlated pairs  $|\text{Corr}(i, j)| = 0$ .

$$C(K, N) = \frac{1}{2} \{1 + \tanh[-\alpha(N) \cdot (K - K_0(N))]\}. \quad (5.10)$$

This describes the transition of  $C(K, N)$  at an average connectivity  $K_0(N)$  which depends only on the system size  $N$ . One finds for the finite size scaling of  $K_0(N)$  that

$$K_0(N) - 2 = a \cdot N^{-\beta} \quad (5.11)$$

with  $a = 3.30 \pm 0.17$  and  $\beta = 0.34 \pm 0.01$  (see Fig. 5.5), whereas the parameter  $\alpha$  scales with system size as

$$\alpha(N) = b \cdot N^\gamma \quad (5.12)$$

with  $b = 0.14 \pm 0.016$  and  $\gamma = 0.41 \pm 0.01$ . This indicates that the transition of  $C(K, N)$  exhibits a sharp decay near the critical connectivity  $K_c$  when the thermodynamic limit  $N \rightarrow \infty$  is approached.

The number of frozen nodes is a decisive quantity for the evolution of adaptive networks. If all nodes are frozen ( $C = 1$ ), as it is typically found for networks with very sparse  $\bar{K}$ , the network is basically irresponsive to signals from the environment and hence can neither process information nor adapt. If, on the other hand,  $C$  vanishes, all nodes exhibit more or less chaotic switching behavior – dynamics becomes completely autonomous and hence again useless for information processing. A finite number of frozen nodes, as it is found near  $K_c$ , enables adaptive response to environmental signals by assignment of new, functional behavior to previously frozen nodes, and also makes sure that global network dynamics avoids the extremes of overly ordered and chaotic regimes. In the following section, we will discuss models of adaptive network evolution by local dynamical rules that lead to emergence

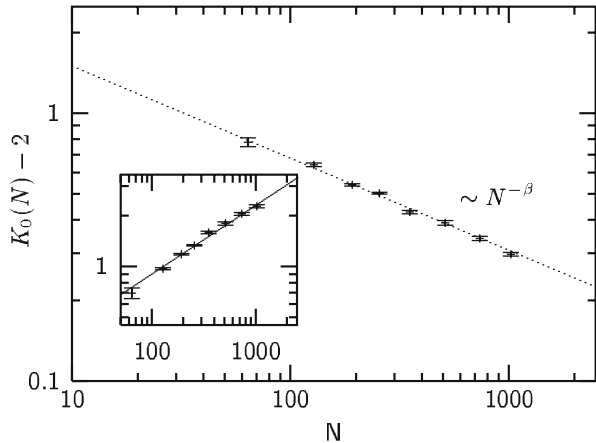


**Fig. 5.5** The finite size scaling of the transition value  $K_0$ , obtained from sigmoidal fits as shown in Fig. 5.4.  $K_0$  approaches  $K_c = 2$  with a scaling law  $\sim N^{-\beta}$ ,  $\beta = 0.34 \pm 0.01$ . The inset shows the scaling behavior of the parameter  $\alpha(N)$ ; one finds  $\alpha(N) \sim N^\gamma$ ,  $\gamma = 0.41 \pm 0.014$

of self-organized critical networks, i.e. networks that evolve to the “optimal” point just at the phase transition from ordered to chaotic dynamics.

### 5.3 Network Self-Organization from Co-evolution of Dynamics and Topology

In this section, we will discuss models of adaptive network self-organization in the context of discrete dynamical networks. The common principle that governs network evolution is a *co-evolution of dynamics and topology from local dynamical rules*: An order parameter of network dynamics is estimated from local measurements (often averaged over a representative number of dynamical update cycles, e.g., over one attractor period of a limit cycle the dynamics converged to, cf. Sect. 5.2.4.1). Based on the measured value of the order parameter, network connectivity and/or the switching behavior of nodes is adapted by local adaptive rules. Usually, there is a time scale separation between frequent dynamical updates and rare rewiring events. After a large number of adaptive cycles, evolution towards a *self-organized critical state* is observed.

#### 5.3.1 Activity-Dependent Rewiring

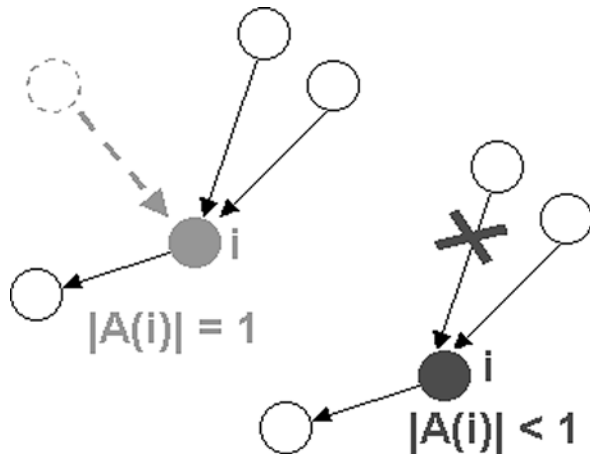
##### 5.3.1.1 Motivation

Living organisms process their information by dynamical systems at multiple levels, e.g. from gene regulatory networks at the cellular level, to neural networks in the central nervous system of multi-cellular organisms. As *complex adaptive systems*, organisms have to deal with the conflicting needs of flexible response to changing environmental cues, while maintaining a reasonable degree of stability in the dynamical networks that process this information. This led to the idea that these systems may have evolved to the “edge of chaos” between ordered and disordered dynamical regimes [40, 50]. In the following, a simple evolutionary mechanism will be introduced [19], based on a local coupling between a dynamical order parameter – the average activity of dynamical units (sites) in RTNs (Eq. 5.8) – and a topological control parameter – the number of inputs a site receives from other units. In a nutshell, the adaptive rule can be summarized as *frozen nodes grow links, active nodes lose links*. This rule abstracts the need for both flexibility and stability of network dynamics. In a gene regulatory network, for example, a frozen gene cannot respond to different inputs it may receive, and hence is practically dysfunctional; the addition of a new regulatory input potentially assigns a new function to this gene. On the other hand, a very active gene will tend to show chaotic switching behavior and may lead to loss of stability in network dynamics – a reduction in input number reduces the probability of this undesirable behavior [78]. Similar demands for a local, homeostatic regulation of activity and connectivity can be expected in neural networks of the nervous system and are supported by experimental evidence [33].

### 5.3.1.2 Model

Let us consider a Random Threshold Network of  $N$  randomly interconnected binary elements as defined in Sect. 5.2.3. In the beginning, network topology is initialized as a directed, random graph with connectivity distributed according to a Poissonian with average connectivity  $K_{ini}$  (cf. Sect. 5.2.1), and  $c_{ij} = +1$  or  $c_{ij} = -1$  with equal probability for non-vanishing links. While network evolution is insensitive to  $K_{ini}$  in general (as will be shown), we choose  $0 < K_{ini} < 3$  in simulations to obtain reasonably fast convergence of the evolutionary dynamics. Network dynamics is iterated according to Eq. (5.5) starting from a random initial state vector  $\Sigma(0) = (\sigma_1(0), \dots, \sigma_N(0))$ , with  $\sigma_i = +1$  or  $\sigma_i = -1$  with equal probability for each  $i$ . After  $T$  iterations, the dynamical trajectory eventually reaches a periodic attractor (limit cycle or fixed point, compare Sect. 5.2.4.1). Then we apply the following local rewiring rule to a randomly selected node  $i$  of the network: **If node  $i$  does not change its state during the attractor, it receives a new non-zero link  $c_{ij}$  from a random node  $j$ . If it changes its state at least once during the attractor, it loses one of its non-zero links  $c_{ij}$ .** Iterating this process leads to a self-organization of the average connectivity of the network. The basic idea of this rewiring rule is sketched schematically in Fig. 5.6, a particular algorithmic realization is provided in Box 5.1.

**Fig. 5.6** The selective criterion leading to topological self-organization: A dynamically frozen site ( $|A(i)| = 1$ ) receives an additional regulatory input, an active site ( $|A(i)| < 1$ ) loses one of its inputs



#### Box 5.1 Adaptive algorithm for activity-dependent rewiring

This box gives an example of an adaptive algorithm that realizes the local rewiring rule “frozen nodes grow links, active nodes lose links” [19]:

1. Choose a random network with an average connectivity  $K_{ini}$ .
2. Choose a random initial state vector  $\Sigma(0) = (\sigma_1(0), \dots, \sigma_N(0))$ .

3. Calculate the new system states  $\Sigma(t)$  according to Eq. (5.2), using parallel update of the  $N$  sites.
4. Once a previous state reappears (a dynamical attractor with period  $\Gamma$  is reached) or otherwise after  $T_{max}$  updates the simulation is stopped. Then, a site  $i$  is chosen at random and its average activity  $A(i)$  during the last  $T = \Gamma$  time steps is determined (in case no attractor is reached,  $T = T_{max}/2$  is chosen).
5. If  $|A(i)| = 1$ ,  $i$  receives a new link  $c_{ij}$  from a site  $j$  selected at random, choosing  $c_{ij} = +1$  or  $-1$  with equal probability. If  $|A(i)| < 1$ , one of the existing non-zero links of site  $i$  is set to zero.
6. Finally, one non-zero entry of the connectivity-matrix is selected at random and its sign reversed.
7. Go to step number 2 and iterate.

### 5.3.1.3 Results

The typical picture arising from the model as defined above is shown in Fig. 5.7 for a system of size  $N = 1,024$ . Independent of the initial connectivity, the system evolves towards a statistically stationary state with an average connectivity  $K_{ev}(N = 1,024) = 2.55 \pm 0.04$ . With varying system size we find that with increasing  $N$  the average connectivity  $\bar{K}$  approaches  $K_c$  (which, for threshold  $h = 0$  as considered here, is found slightly below  $\bar{K} = 2$  [77]), see Fig. 5.8. In particular, one can fit the scaling relationship

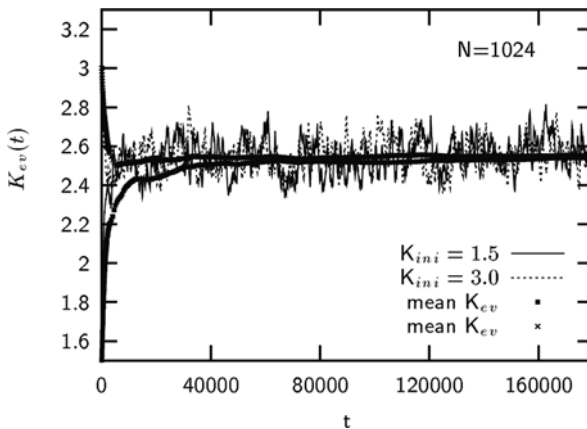


**Fig. 5.7** Evolution of the average connectivity of threshold networks rewired according to the rules described in the text, for  $N = 1,024$  and two different initial connectivities ( $K_{ini} = 1.5$  and  $K_{ini} = 3.0$ ). Independent of the initial conditions chosen at random, the networks evolve to an average connectivity  $K_{ev} = 2.55 \pm 0.04$ . The plot shows the time series and the corresponding cumulative means for  $K_{ev}$ . The evolutionary time  $t$  is discrete, each time step representing a dynamical run on the evolved topology. Individual runs were limited to  $T_{max} = 1,000$  iterations

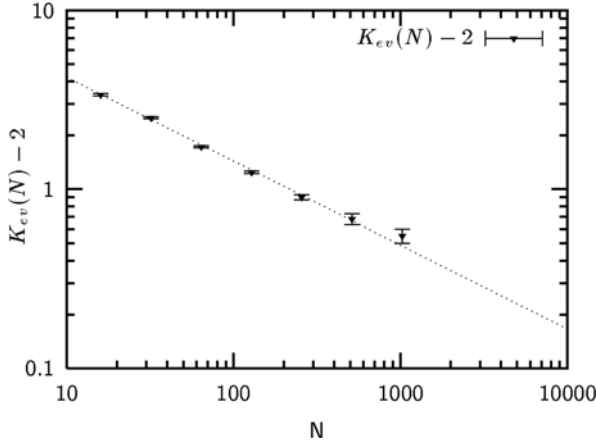


**Fig. 5.8** The average connectivity of the evolved networks converges towards  $K_c$  with a scaling law  $\sim N^{-\delta}$ ,  $\delta = 0.47 \pm 0.01$ . For systems with  $N \leq 256$  the average was taken over  $4 \cdot 10^6$  time steps, for  $N = 512$  and  $N = 1,024$  over  $5 \cdot 10^5$  and  $2.5 \cdot 10^5$  time steps, respectively. Finite size effects from  $T_{max} = 1,000$  may overestimate  $K_{ev}$  for the largest network shown here

$$K_{ev}(N) - 2 = c \cdot N^{-\delta} \quad (5.13)$$

to the measured connectivity values with  $c = 12.4 \pm 0.5$  and  $\delta = 0.47 \pm 0.01$ . In the evolutionary steady state, the average connectivity  $\bar{K}$  of evolving networks exhibits limited fluctuations around the evolutionary mean  $K_{evo}$  which are approximately Gaussian distributed, with a variance vanishing  $\sim 1/N$  [74].

Going beyond averaged topological quantities, one can also measure the degree distributions of inputs and outputs in evolving networks, and compare it to what is expected for random networks (cf. Sect. 5.2.4.3). In finite size networks, substantial deviations from random graphs are found [78]: While the outdegree distribution stays close to the Poissonian of a random graph, evolved in-degree distributions are considerably flatter. For the averaged statistical distribution  $p(K)$  of in-links (Fig. 5.9) of the evolving networks one observes a flat exponential decay

$$p(K) \approx p_0 \cdot \exp[-\alpha K], \quad (5.14)$$

with  $p_0, \alpha = \text{const}$ . This observation indicates that the self-organized network state, at least for finite  $N$ , is substantially different from random networks with the same average connectivity. Since network evolution is based on co-evolutionary adaptation of dynamics and topology by local rewiring rules, this raises the question of whether the evolutionary statistically stationary state exhibits specific characteristics and correlations between dynamical and topological order parameters also on the *global scale*. This is indeed the case for finite  $N$ : If we compare, for example, the frozen component  $C(\bar{K})$  or fraction of “frozen genes” for different values of connectivity fluctuations around the evolutionary mean  $K_{evo}$  (Fig. 5.10), we observe that this curve exhibits a broad plateau where activity is stabilized at intermediate values,

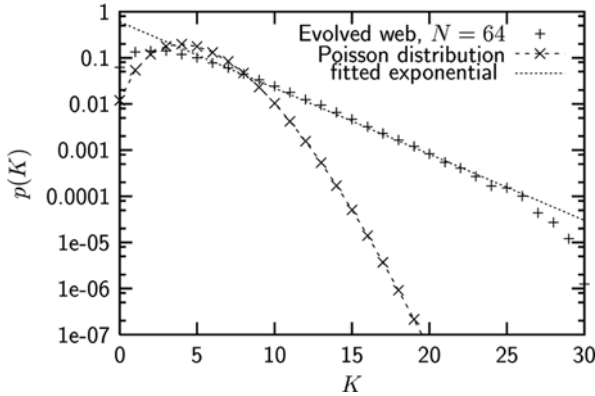


**Fig. 5.9** Statistical distribution  $p(K)$  of the number of inputs  $K$  per node (gene) in the proposed model for a network of size  $N = 64$ . Compared to the Poisson distribution for random networks with  $\bar{K} = 4.46$ , it shows a flatter decay  $\propto \exp[-K]$

with almost step-like boundaries for small and large  $\bar{K}$ , whereas the corresponding curve for random networks is much smoother and decays earlier (compare also Sect. 5.2.4.3 for the phase transition observed in ensembles of random networks). This indicates that coevolution of dynamics and topology extends to a global scale, in spite of local rewiring events and a pronounced time scale separation between dynamical and topological updates.<sup>4</sup>

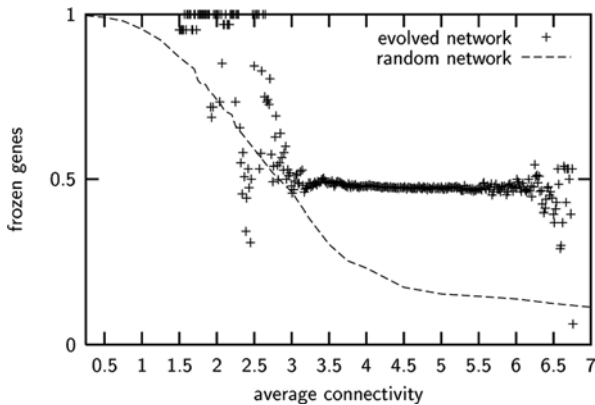


**Fig. 5.10** The frozen component  $C$  (fraction of frozen genes) as a function of the average connectivity for an evolved network of size  $N = 64$  (crosses). The dashed line shows the corresponding curve for random networks

<sup>4</sup> This time scale separation can be easily identified e.g. from step 4 of the adaptive algorithm summarized in Box 5.1: After  $T$  dynamical system updates, one out of  $N$  sites is rewired, hence time scale separation is at the order of  $T \cdot N$ .

Last, let us characterize dynamics *on* the evolving networks, and investigate in how far it may exhibit signatures of self-organized critical behavior even in the finite size networks we studied so far (which, concerning average connectivity, are evidently super-critical). In contrast to random, noise-driven dynamics, where correlations decay fast (typically as an exponential), the self-organized critical state is characterized by non-trivial, long-range correlations in dynamical trajectories. A convenient measure to characterize such long-range correlations is the *power spectrum* of the dynamical time series. Let us consider the autocorrelation function of a time signal  $f(t)$ , defined by

$$R(\tau) = \int_{-\infty}^{+\infty} f(t)f(t - \tau) dt. \quad (5.15)$$

The power spectrum  $G(f)$  is the Fourier transform of the autocorrelation function, i.e.

$$G(f) = \int_{-\infty}^{+\infty} R(\tau)e^{-2\pi if\tau} d\tau. \quad (5.16)$$

In the case of time-discrete systems, the integrals are replaced by the corresponding sums. For strongly (auto-)correlated systems, e.g. near the critical point, we typically expect a flat decay of the power spectrum  $G(f) \sim 1/f^\alpha$  with  $\alpha \approx 1$ , while for a random walk, e.g., we would obtain  $\alpha = 2$ . The dynamical order parameter that we investigate is the *global average activity* at evolutionary time step  $t$ :

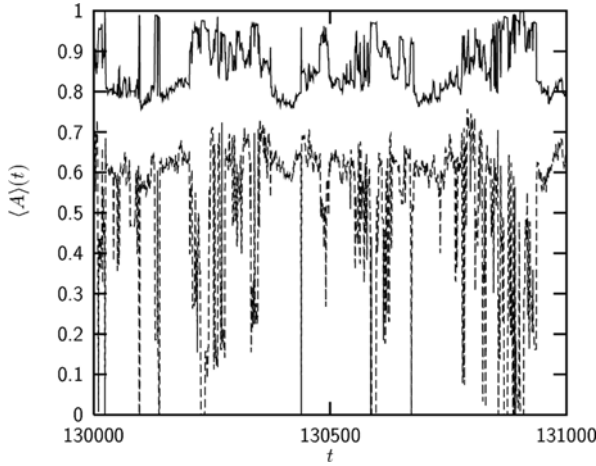
$$\langle A \rangle(t) = \left| \frac{1}{N} \sum_{i=1}^N A_i(t) \right|. \quad (5.17)$$

Figure 5.11 shows a typical snapshot of the time series of  $\langle A \rangle$  on evolving networks, the power spectrum is shown in Fig. 5.12. A least squares fit yields  $G(f) \sim 1/f^\alpha$  with  $\alpha = 1.298$  for the global average activity, i.e. a clear indication of long-range correlations in dynamics [74]. Other measures of global dynamics also show evidence for criticality, for example, the statistical distribution of attractor periods is scale-free, as will be discussed in Sect. 5.3.3 for a RBN variant of the model.

The self-organization towards criticality observed in this model is different from other known mechanisms exhibiting the amazingly general phenomenon of self-organized criticality (SOC) [7, 8, 71, 84]. Our model introduces a (new, and interestingly different) type of mechanism by which a system self-organizes towards criticality, here  $K \rightarrow K_c$ . This class of mechanisms lifts the notions of SOC to a new level. In particular, it exhibits considerable robustness against noise in the system. The main mechanism here is based on a topological phase transition in dynamical networks.

In addition to the rewiring algorithm as described in this chapter, a number of different versions of the model were tested. Including the transient in the measurement





**Fig. 5.11** Time series of the global average activity  $\langle A \rangle$  (arbitrary time window of the evolutionary process). *Upper curve*: Signal averaged over the whole network, *lower curve*: Signal averaged over non-frozen nodes only

of the average activity  $A(i)$  results in a similar overall behavior (where we allowed a few time steps for the transient to decouple from initial conditions). Another version succeeds using the correlation between two sites instead of  $A(i)$  as a mutation criterion (this rule could be called “anti-Hebbian” as in the context of neural network learning). In addition, this version was further changed allowing different locations of mutated links, both, between the tested sites or just at one of the nodes. All these different realizations exhibit the same basic behavior as found for the model above.

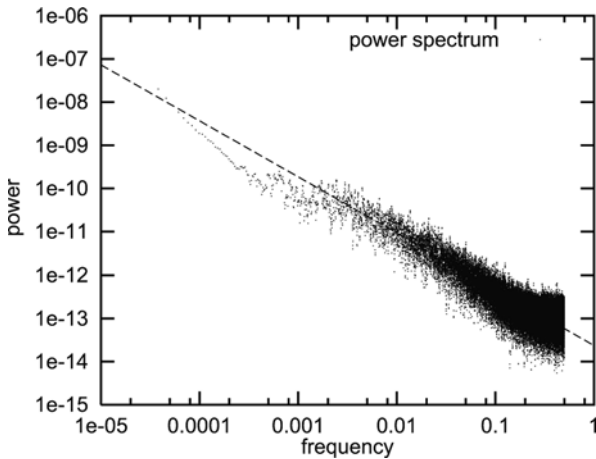


**Fig. 5.12** Power spectrum of the global average activity  $\langle A \rangle$  over  $10^5$  evolutionary time steps, averaged over all network sites (compare *upper curve* in Fig. 5.11, double-logarithmic plot. The *dashed line* has slope  $-1.298$ )

Thus, the proposed mechanism exhibits considerable robustness. Interestingly, it has been shown that this mechanism leads to robust topological and dynamical self-organization also in other classes of dynamical networks. In particular, Teuscher and Sanchez [87] showed that this rule can be generalized to Turing neural networks and drives network evolution to  $K_c = 2$  in the limit of large  $N$ .

In the next subsection, we will discuss an extension of the model that includes adaptation of thresholds in RTN, in addition to rewiring of links. This extension still exhibits robust self-organization as in the original model, however, exhibits several interesting new features, namely, symmetry breaking of evolutionary attractors, and correlation of dynamical and topological diversity.

### 5.3.2 Adaptive Thresholds – Time Scale Separation Leads to Complex Topologies

So far, we assumed that dynamical units in the networks are homogeneous (identical) with respect to their switching behavior, which for real world networks usually is a quite unrealistic assumption. Furthermore, recent studies have shown that inhomogeneity of thresholds leads to new and unexpected phenomena in RTNs, e.g. an order-disorder transition induced by *correlations* between thresholds and input number of nodes [75]. In the general case of inhomogeneous thresholds, we have to modify Eq. (5.5) such that

$$f_i(t) = \sum_{j=1}^N c_{ij} \sigma_j(t) + h_i, \quad (5.18)$$

where the indexed threshold  $h_i$  now takes into account that thresholds can vary from node to node. The only restriction we impose is  $h_i \leq 0$ , to make activation, i.e.  $\sigma_i = +1$ , more difficult.

We now introduce a minimal model linking regulation of activation thresholds and rewiring of network nodes in RTNs to local measurements of a dynamical order parameter [76]. Adaptation of thresholds opens up for the possibility of units that become heterogeneous with respect to their *dynamical* properties: Nodes with high thresholds are inert and switch their state only for few input configurations (similar to the effect of canalizing functions in RBNs), whereas nodes with low thresholds are more likely to switch. A new control parameter  $p \in [0, 1]$  determines the probability of rewiring vs. threshold adaptations. In particular, the activity  $A(i)$  of a site  $i$  can be controlled in two ways: If  $i$  is frozen, it can increase the probability to change its state by either increasing its number of inputs  $k_i \rightarrow k_i + 1$ , or by making its threshold  $h_i \leq 0$  less negative, i.e.  $|h_i| \rightarrow |h_i| - 1$ . If  $i$  is active, it can reduce its activity by adapting either  $k_i \rightarrow k_i - 1$  or  $|h_i| \rightarrow |h_i| + 1$ . To realize this adaptive scheme, we have to modify step 4 in the adaptive algorithm of Box 5.1: **A site  $i$  is chosen at random and its average activity  $A(i)$  during the last  $T = \Gamma$  time steps is determined (in case no attractor is reached,  $T = T_{max}/2$  is chosen). If  $|A(i)| < 1$ , then  $k_i \rightarrow k_i - 1$  with probability  $p$  (removal of one**

**randomly selected input). With probability  $1 - p$ , adapt  $|h_i| \rightarrow |h_i| + 1$  instead. If  $|A(i)| = 1$ , then  $k_i \rightarrow k_i + 1$  with probability  $p$  (addition of a new input from a randomly selected site). With probability  $1 - p$ , adapt  $|h_i| \rightarrow |h_i| - 1$  instead. If  $h_i = 0$ , let its value unchanged.** If the control parameter  $p$  takes values  $p > 1/2$ , rewiring of nodes is favored, whereas for  $p < 1/2$  threshold adaptations are more likely. Notice that the model discussed in the last subsection is contained as the limiting case  $p = 1$  (rewiring only and  $h_i = const. = 0$  for all sites).

*Results.* After a large number of adaptive cycles, networks self-organize into a *global* evolutionary steady state. An example is shown in Fig. 5.13 for networks with  $N = 512$ : starting from an initial value  $\bar{K}_{ini} = 1$ , the networks' average connectivity  $\bar{K}$  first increases, and then saturates around a stationary mean value  $\bar{K}_{evo}$ ; similar observations are made for the average threshold  $\bar{h}$  (Fig. 5.13, lower panel). The non-equilibrium nature of the system manifests itself in limited fluctuations of both  $\bar{K}$  and  $\bar{h}$  around  $\bar{K}_{evo}$  and  $\bar{h}_{evo}$ . Regarding the dependence of  $\bar{K}$  with respect to  $p$ , we make the interesting observation that it changes non-monotonically. Two cases can be distinguished: When  $p = 1$ ,  $\bar{K}$  stabilizes at a very sparse mean value  $\bar{K}_{evo}$ , e.g. for  $N = 512$  at  $\bar{K}_{evo} = 2.664 \pm 0.005$ . When  $p < 1$ , the symmetry of this evolutionary steady state is broken. Now,  $\bar{K}$  converges to a much higher mean value  $\bar{K}_{evo} \approx 43.5 \pm 0.3$  (for  $N = 512$ ), however, the particular value which is finally reached is *independent of  $p$* . On the other hand, *convergence times  $T_{con}$*  needed to reach the steady state are strongly influenced by  $p$ :  $T_{con}(p)$  diverges when  $p$

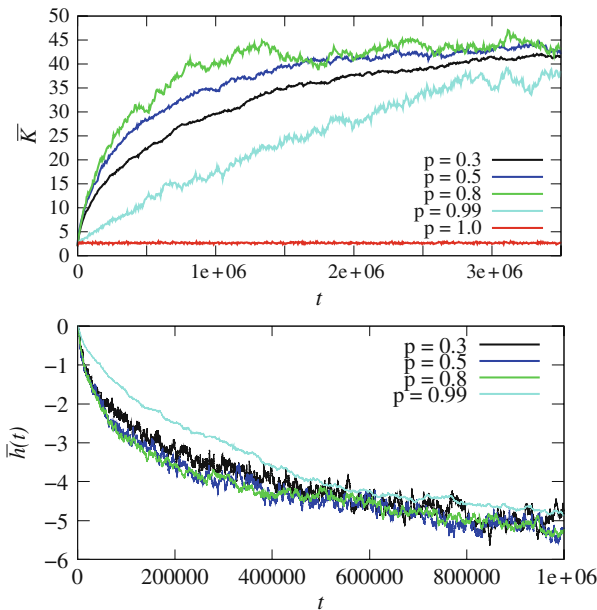


**Fig. 5.13** Upper panel: Evolution of the average connectivity  $\bar{K}$  of threshold networks, using the adaptive algorithm (cf. Fig. 5.1) for  $N = 512$  and initial connectivity  $\bar{K}_{ini} = 1$ . Time series for five different values of  $p$  are shown. Lower panel: The same for the average threshold  $\bar{h}$

approaches 1 (compare Fig. 5.2 for  $p = 0.99$ ). We conclude that  $p$  determines the *adaptive time scale*. This is also reflected by the stationary in-degree distributions  $p(k_{in})$  that vary considerably with  $p$  (Fig. 5.14); when  $p \rightarrow 1$ , these distributions become very broad. The numerical data suggest that a power law

$$\lim_{p \rightarrow 1} p(k_{in}) \propto k_{in}^{-\gamma} \quad (5.19)$$

with  $\gamma \approx 3/4 \pm 0.03$  is approached in this limit (cf. Fig. 5.4, dashed line). At the same time, it is interesting to notice that the evolved out-degree distributions are much narrower and completely insensitive to  $p$  (Fig. 5.14, data points without lines). Hence, we make the interesting observation of a highly robust self-organization and homeostatic regulation of the average wiring density, while, at the same time in the limit  $p \rightarrow 1$ , time scale separation between frequent rewiring and rare threshold adaptation leads to emergence of complex, heterogeneous topologies, as reflected in the broad distribution of input numbers approaching a power law. Obviously, we have a non-trivial coevolutionary dynamics in the limit  $p \rightarrow 1$  which is significantly different from the limit of small  $p$ . This is also indicated by the emergence of strong correlations between input number and thresholds in this limit (see the steep increase of the curves for  $p > 0.5$  in Fig. 5.15), while in the limit of small  $p$  correlations are weak.

To summarize, we find that coevolution of both rewiring and threshold adaptation with the dynamical activity on RTNs leads to a number of interesting new effects: We find spontaneous symmetry breaking into a new class of adaptive networks that is characterized by increased heterogeneity in wiring topologies and emergence of correlations between thresholds and input numbers. At the same time, we find a highly robust regulation of the average wiring density which is independent of  $p$  for any  $p < 1$ .

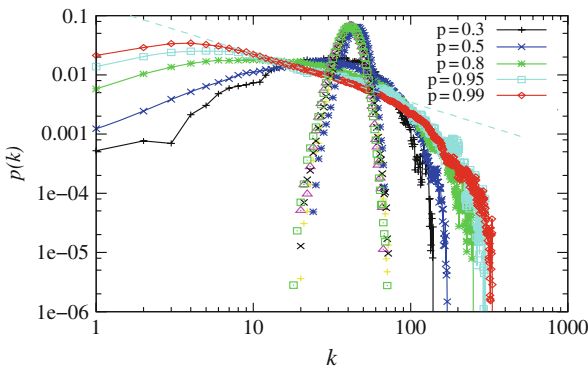


**Fig. 5.14** *Line-pointed curves*: in-degree distributions of evolved networks, *data points only*: the corresponding out-degree distributions ( $\Delta$ )  $p = 0.3$ , (+)  $p = 0.5$ , (x)  $p = 0.8$ , (\*)  $p = 0.95$ , (squares)  $p = 0.99$ ). Statistics was gathered over  $10^6$  evolutionary steps, after a transient of  $4 \cdot 10^6$  steps. Networks had size  $N = 512$ . The *dashed line* has slope  $-3/4$

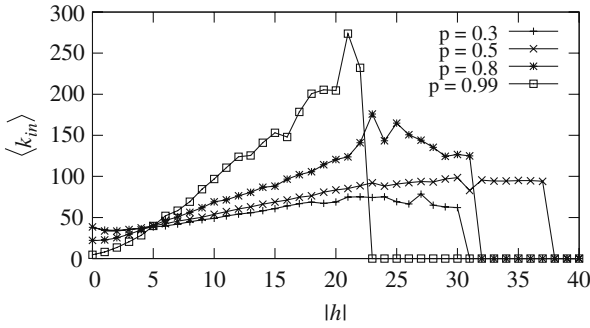


**Fig. 5.15** Average number  $\langle k_{in} \rangle$  of inputs for a given node in evolving networks, as a function of the respective nodes (absolute) threshold  $|h|$ . Statistics was taken over  $10^6$  rewiring steps, after a transient of  $4 \cdot 10^6$  steps. For all values  $p < 1$ , a clear positive correlation between  $\bar{k}_{in}$  and  $|h|$  is found

In the next subsection, we will discuss another generalization of the adaptive, coevolutionary scheme of activity-dependent rewiring to Random Boolean Networks, which was introduced by Liu and Basler [53].

### 5.3.3 Extension to Random Boolean Networks

Activity-dependent rewiring was originally introduced for Random Threshold Networks, as discussed in Sect. 5.3.1.2, the basic adaptive scheme, however, can be generalized to other classes of dynamical systems. Since RTNs are a subclass of Random Boolean Networks, one possible direction of generalization is to apply this coevolutionary, adaptive rule to RBNs. Compared to RTNs, rewiring by local dynamical rules in RBN comes with an additional complication: While in RTNs the dynamical transition rule is the same for all network sites (the evaluation of the weighted sum of regulatory inputs, cf. Eq. 5.6), switching of network nodes in RBNs is governed by individual logical functions that vary from node to node and depend on the input number  $k$ . If, for example, we have a node with two inputs and a logical AND function of these two inputs assigned (compare the example in Fig. 5.1), there does not exist a well-defined mapping that would assign a new logical function to this node in the case we change its input number to  $k = 1$  or  $k = 3$ .

Liu and Bassler [53] suggested two variants of activity-dependent rewiring to overcome the problem associated to the reassignment of logical functions: in the first variant, only the node that is rewired at evolutionary time step  $t$  is assigned a new logical function which is randomly drawn out of the  $2^{2^k}$  possible Boolean functions of  $k$  inputs (where  $k$  is the new input number after rewiring). The adaptive algorithm that was applied in this study is summarized in Box 5.2.

### Box 5.2 Adaptive algorithm for activity-dependent rewiring in RBN

1. Start with a homogeneous RBN,  $G(N, K_0)$  with uniform in-degree connectivity  $K_i = K_0$  for all  $N$ , and generate a random Boolean function  $f_i$  for each node  $i$ .
2. Choose a random initial system state  $\Sigma(0)$ . Update the state using Eq. (5.4) and find the dynamical attractor.
3. Choose a node  $i$  at random and determine its average activity  $A(i)$  over the attractor.
4. Change the network topology by rewiring the connections to the node chosen in the previous step. If it is frozen, then a new incoming link from a randomly selected node  $j$  is added to it. If it is active, then one of its existing links is randomly selected and removed.
5. The Boolean functions of network are regenerated. Two different methods have been used:
  - Annealed model: A new Boolean function is generated for every node of the network.
  - Quenched model: A new Boolean function is generated only for the chosen node  $i$ , while the others remain what they were previously.
6. Return to step 2.

For simplicity, all random Boolean functions are generated with  $p = 1/2$ , and therefore all Boolean functions with the same in-degree are equally likely to be generated.

*Results.* Liu and Bassler show that for both variants of the model, robust self-organization of network topology is found. Independent from the initial network realization, network evolution always converges to a characteristic average connectivity  $K_{ev}(N)$ . Graph (a) of Fig. 5.16 shows the evolution of the average in-degree connectivity  $\bar{K}$  for networks of size  $N = 30$  in the annealed variant of the model, with results obtained by beginning with networks with different uniform connectivity  $K_0 = 2, 3, 4$ , and 5. Each curve is the average of 15000 independent realizations of the network evolution. All curves approach the same final statistical steady state that has an average in-degree connectivity  $\langle \bar{K} \rangle = 3.06$ . The steady state value of  $\langle \bar{K} \rangle$  depends on the size of the system as shown in graph (b) of Fig. 5.16. Starting with networks that all have the same initial uniform connectivity  $K_0 = 4$ , but which have different size  $N = 30, 50$ , and 100, one finds that larger networks evolve to steady states with smaller values of  $\langle \bar{K} \rangle$ .

Given the steady state value  $\langle \bar{K} \rangle = 2$  in the large network limit  $N \rightarrow \infty$ , Liu and Bassler also studied the finite-size effects in the model. They found that the values of  $\langle \bar{K}(N) \rangle$  for finite  $N$  obey the scaling function

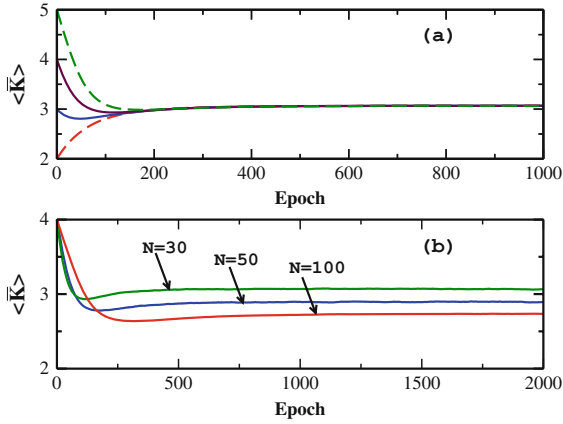


**Fig. 5.16** (a). Evolution of the ensemble averaged in-degree connectivity in the annealed model, as studied by Liu and Bassler [53], for networks of size  $N = 30$ . The networks in each ensemble initially start from different uniform connectivity,  $K_0 = 2, 3, 4$ , and  $5$ , but reach a same statistical steady state  $\langle \bar{K} \rangle = 3.06$ . (b). Evolution of ensemble averaged in-degree connectivity for networks of three different size  $N = 30, 50$ , and  $100$  in the annealed model

$$\langle \bar{K}(N) \rangle - 2 = c N^{-\delta}. \tag{5.20}$$

Fitting the data to this function, we find that the coefficient is  $c = 2.50 \pm 0.06$  and the exponent is  $\delta = 0.264 \pm 0.005$ . Thus the value of  $\langle \bar{K}(N) \rangle$  is always larger than 2 for finite  $N$ . Note that steady state values of the average connectivity in RTNs have a similar scaling form, but with slightly different values of the scaling parameters (cf. Sect. 5.3.1.3, Eq. 5.13).

In order to probe the dynamical nature of evolved steady states the authors computed the distribution  $P(\Gamma)$  of steady state attractor period  $\Gamma$  in the ensemble of RBNs simulated. The distribution has a broad, power-law behavior for both the

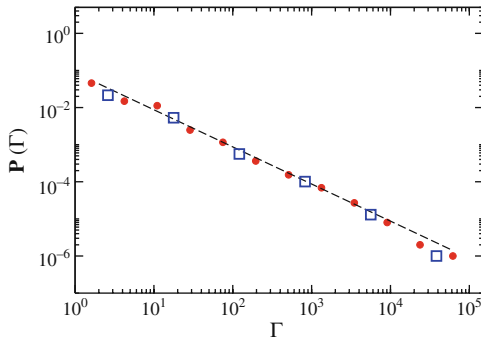


**Fig. 5.17** Power law distribution of steady state attractor period  $\Gamma$  in both annealed (*circle*) and quenched (*square*) models as studied by Liu and Bassler [53], for  $N = 200$  systems. The *dashed straight line* has a slope of 1.0

annealed and quenched variants of the model. Figure 5.17 shows the results for networks with  $N = 200$ . A power-law distribution of attractor periods is a typical signature of critical dynamics, hence, similar to the results discussed in Sect. 5.3.1.3 for the self-organization of the global average activity, this finding indicates that *dynamics* exhibits close-to critical behavior already for finite size networks, while *topological* criticality is attained in the limit of large  $N$ .

To summarize, the results of this study give strong evidence that the local, adaptive coevolutionary principle *frozen nodes grow links, active nodes lose links* leads to robust self-organization not only in RTNs, but also in the more general class of RBNs, and hence has the potential to be generalized to large classes of dynamical systems.

### 5.3.4 Correlation-Based Rewiring in Neural Networks

In this section, we will review a different adaptive coevolutionary scheme of network self-organization which is based on the basic paradigm *correlated activity connects, decorrelated activity disconnects*. This local, topology-evolving rule is inspired by the idea of *Hebbian learning* in neural networks [38], and, consequently, was studied first for discrete neural networks with architectural and dynamical constraints motivated by corresponding observations in the brain [18]. In particular, an explicit parameterization of space on a two-dimensional grid is given, and dynamics is not deterministic any more, in contrast to the models discussed in the previous sections. The core result of this study is that network self-organization by correlation-driven rewiring is robust even when spatial constraints are present and dynamics is affected by noise. Correlation-driven rewiring can be considered as a natural extension of the basic, activity-driven rewiring, as it exploits long range correlations naturally emerging near phase transitions, and thereby is particularly suited for neural networks where information processing takes place typically in form of correlated activity. Let us now briefly motivate the correlation based self-organization in the context of neural networks.

Neural networks with asymmetric connectivity patterns often exhibit regimes of chaotic dynamics [63]. In networks whose central function is information transfer, these regimes would instantly render them useless. Consider, for example, model neural networks with asymmetric synaptic couplings, where a percolation transition between regimes of ordered and disordered dynamics is known [48]. In the disordered phase, which occurs for densely connected networks, already small perturbations percolate through the networks.<sup>5</sup> In such networks, developmental processes that change connectivity always face the risk of driving the network into the highly connected regime (where chaotic dynamics prevails), as long as no explicit mechanism is given that controls the global degree of connectivity.

---

<sup>5</sup> This is reminiscent of avalanche-like propagation of activity in the brain which is observed in some diseases of the central nervous system [81].



In a correlation-based rewiring rule we will exploit that also the average correlation between the activities of two neurons contains information about global order parameter of network dynamics. The network can then use this approximate order parameter to guide the developmental rule. A possible adaptive scheme is that new synaptic connections preferentially grow between correlated neurons, as suggested by the early ideas of Hebb [38] and the observation of activity-dependent neural development [33, 62, 69, 89]. In the remainder of this section let us recapitulate this problem in the framework of a specific toy model [18]. First a neural network model with a simple mechanism of synaptic development is defined. Then, the interplay of dynamics on the network with dynamics of the network topology is modeled. Finally, robustness of self-organizing processes in this model and possible implications for biological systems are discussed.

### 5.3.4.1 Model

Let us consider a two-dimensional neural network with random asymmetric weights on the lattice. The neighborhood of each neuron is chosen as its Moore neighborhood with eight neighbors.<sup>6</sup> The weights  $c_{ij}$  are randomly drawn from a uniform distribution  $c_{ij} \in [-1, +1]$  and are nonzero between neighbors, only. Note that weights  $c_{ij}$  are asymmetric, i.e., in general,  $c_{ij} \neq c_{ji}$ . Within the neighborhood of a node, a fraction of its weights  $c_{ij}$  may be set to 0. The network consists of  $N$  neurons with states  $\sigma_i = \pm 1$  which are updated in parallel with a stochastic Little dynamics on the basis of inputs received from the neighbor neurons at the previous time step:

$$\sigma_i(t+1) = \begin{cases} +1 & \text{with probability } g_\beta(f_i(t)) \\ -1 & \text{with probability } 1 - g_\beta(f_i(t)) \end{cases} \quad (5.21)$$

where

$$g_\beta(f_i(t)) = \frac{1}{1 + e^{-2\beta f_i(t)}} \quad (5.22)$$

with the inverse temperature  $\beta$ . The transfer function  $f_i(t)$  is evaluated according to Eq. 5.18, that defines dynamics of threshold units with individually assigned thresholds. The threshold is chosen here as  $h_i = -0.1 + \gamma$  and includes a small random noise term  $\gamma$  from a Gaussian of width  $\varepsilon$ . This noise term is motivated by the slow fluctuations observed in biological neural systems [1, 2].

---

<sup>6</sup> The choice of the type of neighborhood is not critical, however, here the Moore neighborhood is more convenient than the von Neumann type since, in the latter case, the critical link density (fraction of nonzero weights) at the percolation threshold accidentally coincides with the attractor of the trivial developmental rule of producing a link with  $p = 0.5$ . In general, also random sparse neighborhoods would work as demonstrated in [21].

The second part of the model is a slow change of the topology of the network by local rewiring of synaptic weights: If the activity of two neighbor neurons is on average highly correlated (or anticorrelated), they will obtain a common link. If their activity on average is less correlated, they will lose their common link. The degree of correlation in the dynamics of pairs of nodes is quantified by the *average correlation*, as defined in Eq. (5.9) in Sect. 5.2.4.2. The full model dynamics is then realized by the algorithm summarized in Box 5.3.

**Box 5.3 Adaptive algorithm for correlation-dependent rewiring in neural networks**

1. Start with a random network with an average connectivity (number of nonzero weights per neuron)  $K_{ini}$  and a random initial state vector  $\Sigma(0) = (\sigma_1(0), \dots, \sigma_N(0))$ .
2. For each neuron  $i$ , choose a random threshold  $h_i$  from a Gaussian distribution of width  $\varepsilon$  and mean  $\mu$ .
3. Starting from the initial state, calculate the new system state applying Eq. (5.21) using parallel update. Iterate this for  $\tau$  time steps.
4. Randomly choose one neuron  $i$  and one of its neighbors  $j$  and determine the average correlation according to Eq. (5.8) over the last  $\tau/2$  time steps. (Alternatively, the correlation can be obtained from a synaptic variable providing a moving average at any given time).
5. If  $|\text{Corr}(i, j)|$  is larger than a given threshold  $\alpha$ ,  $i$  receives a new link  $c_{ij}$  from site  $j$  with a weight chosen randomly from the interval  $c_{ij} \in [-1, 1]$ . If  $|\text{Corr}(i, j)| \leq \alpha$ , the link  $c_{ij}$  is set to 0 (if nonzero).
6. Go to step 2 and iterate, using the current state of the network as new initial state.

The dynamics of this network is continuous in time, with neuron update on a fast time scale and topology update of the weights on a well-separated slow “synaptic plasticity” time scale. Note that the topology-changing rule does not involve any global knowledge, e.g., about attractors.

**5.3.4.2 Results**

Independent of the initial conditions the networks evolve to a specific average connectivity. Parameters are  $\beta = 25$ ,  $\epsilon = 0.1$ , a correlation cutoff  $\alpha = 0.8$ , and an averaging time window of  $\tau = 200$ . One observes that the continuous network dynamics, including the slow local change of the topology, results in a convergence of the average connectivity of the network to a characteristic value which is independent of initial conditions.

Finite size scaling of the resulting average connectivity indicates the convergence towards a characteristic value for large network size  $N$  and exhibits the scaling relationship

$$K_{ev}(N) = aN^{-\delta} + b \quad (5.23)$$

with  $a = 1.2 \pm 0.4$ ,  $\delta = 0.86 \pm 0.07$ , and  $b = 2.24 \pm 0.03$ . Thus, in the large system size limit  $N \rightarrow \infty$  the networks evolve towards  $K_{ev}^{\infty} = 2.24 \pm 0.03$ . The self-organization towards a specific average connectivity is largely insensitive to thermal noise of the network dynamics, up to  $\approx 10\%$  of thermal switching errors (or  $\beta > 10$ ) of the neurons. This indicates that the structure of a given dynamical attractor is robust against a large degree of noise. Figure 5.18 shows the evolved average connectivity as a function of the inverse temperature  $\beta$ .

While the stability of dynamical attractors on an intermediate time scale is an important requirement for the local sampling of neural correlation, on the long time scale of global topological changes, switching between attractors is necessary to ensure ergodicity at the attractor sampling level. The second source of noise, the slow random change in neural thresholds as defined in step (2) of the algorithm, is closely related to such transitions between attractors. While, in general, the model converges also when choosing some arbitrary fixed threshold  $h$  and omitting step (2) from the algorithm, a small threshold noise facilitates transitions between limit cycle attractors [61] and thus improves sampling over all attractors of a network, resulting in an overall increased speed and robustness of the convergence. An asynchronous change of the threshold  $h_i$ , updating one random  $h_i$  after completing one sweep (time step) of the network, leads to similar results as the parallel rule defined above.

The basic mechanism of the observed self-organization in this system is the weak coupling of topological change to an order parameter of the global dynamical state of the network, and thus is different from the mechanism of extremal dynamics, underlying many prominent models of self-organized criticality [7, 8]. To illustrate this, let us for a moment consider the absolute average correlation  $|\text{Corr}(i, j)|$  of two neurons which is the parameter used as a criterion for the rewiring process. It can be shown that this quantity undergoes a phase transition depending on the average

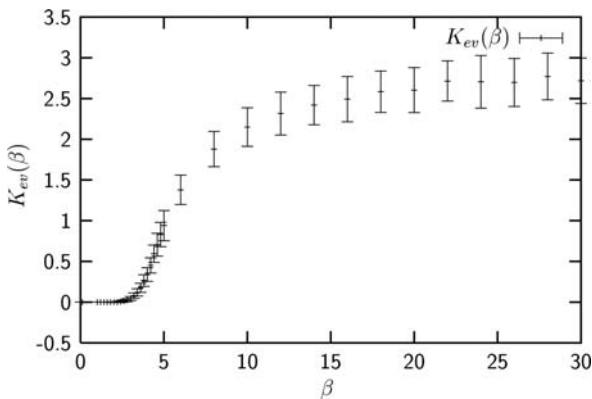


**Fig. 5.18** Evolved average connectivity  $K_{ev}$  as a function of the inverse temperature  $\beta$ . Each point is averaged over  $10^5$  time steps in a network of size  $N = 64$  and  $\alpha = 0.5$ . After Bornholdt and Röhl [18]

connectivity  $\bar{K}$  which is similar to the transition of the frozen component observed in RTN (Fig. 5.4, cf. Sect. 5.2.4.3). Note that the correlation is large for networks with small connectivity, and small for networks that are densely connected. The rewiring rule balances between these two regimes: For high correlation, it is more likely that a link is created, at low correlation, links are vanishing. The balance is reached most likely in the region of the curve where the slope reaches its maximum, as here the observed correlation reacts most sensitively to connectivity changes. As the steep portion of the correlation curve occurs in a region of small connectivities where also the critical connectivity  $K_c \approx 2$  of the network is located, this makes the correlation measure sensitive to the global dynamical state of the network and potentially useful as an approximation of the order parameter. Synaptic development dependent on averaged correlation between neurons can thus obtain approximate information about the global dynamical state of the network as is realized in the above toy model with a simple implementation on the basis of a threshold  $\alpha$ . The exact choice of the threshold  $\alpha$  is not critical, which can be seen from the histogram of the absolute correlation shown in Fig. 5.19 for a typical run of the model. Correlations appear to cluster near high and near low values such that the cutoff can be placed anywhere in between the two regimes. Even a threshold value close to 1, as compared with the correlation cutoff  $\alpha = 0.8$  used in the simulations here, only leads to a minor shift in  $K_{ev}$  and does not change the overall behavior.

Up to now we focused on changes of the network structure as a result of the dynamics on the network. A further aspect is how the structural changes affect the dynamics on the network itself. Do also dynamical observables of the networks self-organize as a result of the observed convergence of the network structure? An interesting quantity in this respect is the average length of periodic attractors.

Indeed, this dynamical observable of the network dynamics converges to a specific value independent of the initial network, similarly to the convergence of the structural parameter  $\bar{K}$  considered earlier. From the  $\bar{K}$  dependency of the neural

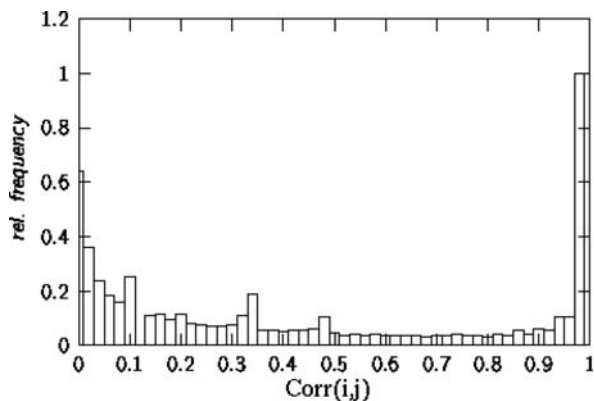


**Fig. 5.19** Histogram of  $\text{Corr}(i, j)$  for a network evolving in time, with  $N = 64$  and  $\beta = 10$ , taken over a run of  $4 \times 10^5$  time steps, according to the model of Bornholdt and Röhl [18]

pair correlation we have seen above that the rewiring criterion tends to favor connectivities near the critical connectivity of the network. Does also the evolved average attractor length relate to critical properties of the percolation transition? An approximate measure of this aspect is the finite size scaling of the evolved average period.

For static networks we find that the attractor lengths typically scale exponentially with  $N$  in the overcritical regime, but less than linearly in the ordered regime. For the evolved connectivity  $K_{ev}$  in our model, we observe scaling close to criticality. Large evolved networks exhibit relatively short attractors, which otherwise for random networks in the overcritical regime could only be achieved by fine tuning. The self-organizing model studied here evolves non-chaotic networks without the need for parameter tuning.

In a continuously running network, robust self-organization of the network towards the percolation transition between ordered and disordered dynamics is observed, independent of initial conditions and robust against thermal noise. The basic model is robust against changes in the details of the algorithm. We conclude that a weak coupling of the rewiring process to an approximate measurement of an order parameter of the global dynamics is sufficient for a robust self-organization towards criticality. In particular, the order parameter has been estimated solely from information available on the single synapse level via time averaging of correlated neural activities.

## 5.4 Summary and Outlook

We reviewed models of topological network self-organization by *local dynamical rules*. Two paradigms of local co-evolutionary adaptation were applied to discrete dynamical networks: The principle of *activity-dependent rewiring* (active nodes lose links, frozen nodes acquire new links), and the principle of *correlation-dependent rewiring* (nodes with correlated activity connect, decorrelated nodes disconnect). Both principles lead to robust self-organization of *global* network topology and – dynamics, without need for parameter tuning. Adaptive networks are strikingly different from random networks: they evolve inhomogeneous topologies and broad plateaus of homeostatic regulation, dynamical activity exhibits  $1/f$  noise and attractor periods obey a scale-free distribution. The proposed co-evolutionary mechanism of topological self-organization is robust against noise and does not depend on the details of dynamical transition rules. Using finite-size scaling, it was shown that networks converge to a self-organized critical state in the thermodynamic limit.

The proposed mechanisms of coevolutionary adaptation in dynamical networks are very robust against changes in details of the local rewiring rules – in particular, they only require a local estimate of some dynamical order parameter in order to achieve network adaptation to criticality.

A classical route to self-organized criticality is the feedback of an order parameter onto local dynamics of a system [85]. The local rewiring rules considered here extend this idea to using only approximate local estimates of a global order

parameter. As seen in the examples above, locally measured averages prove to be sufficient for self-organized criticality. In particular, in the presence of a time-scale separation between fast dynamics on the networks and slow topology evolution, the evolutionary steady state naturally provides a quasi-ergodic sampling of the phase space near the critical state, such that accurate order parameter values are not necessary. In the models considered in this review, an estimate of the order parameter is achieved by local averaging over the switching activity of single nodes, or over the dynamical correlation of pairs of nodes.

A number of open questions remains to be addressed in the context of the class of adaptive networks considered here. The robust network self-organization observed in the models, approaching criticality in the limit of large  $N$ , is far from being understood in detail. With regard to dynamics, evolving networks exhibit pronounced differences to random networks with comparable connectivity. In particular, the frozen component exhibits for finite  $N$  a plateau around the evolutionary mean  $K_{evo}$ , with step-like discontinuities when the average wiring density substantially departs from  $K_{evo}$  (Fig. 5.10); for comparison, the corresponding curves for random networks show a smooth decay. This may suggest that the self-organized critical state rather exhibits characteristics of a first order phase transition, while order parameters in random discrete dynamical networks typically exhibit second order transitions at  $K_c$ . With regard to topology, deviations from random networks become particularly pronounced when dynamical units are allowed to diversify with respect to their switching behavior during evolution, leading to symmetry breaking and emergence of scale-free in-degree distributions; again, these observations are hard to explain in the context of the traditional statistical mechanics approach based on random ensembles of networks.

In the studies reviewed in this chapter, evolving networks were treated as completely autonomous systems, without coupling to an external environment. An important step in future research will be to introduce network-environment interaction and study network evolution under the influence of external signals or perturbations; this also connects to the particularities of information processing in self-organized critical networks, and the idea of optimal adaptation at the “edge of chaos” [15].

Finally, let us widen the scope of these models beyond their theoretical value, and discuss possible applications.

On the one hand, they represent prototypical models of self-organized critical dynamical networks, toy models that demonstrate possible mechanisms for dynamical networks to adapt to criticality. On the other hand, these mechanisms are not limited to the extremely simple toy models discussed here, and may themselves occur in natural systems. They do not depend on fine-tuning of parameters or details of the implementation, and they are robust against noise. This is contrary to standard mechanisms of self-organized criticality [7, 8] which are sensitive to noise [80] and, therefore, not easily applied to natural systems. Network self-organization as reviewed above, however, is itself defined on the basis of stochastic dynamical operations (update of randomly selected links, noisy local measurement of order

parameter, for example). We therefore expect that these mechanisms can occur in natural systems quite easily.

A strong need for adaptive mechanisms is present in nervous systems, where assemblies of neurons need to self-adjust their activity levels, as well as their connectivity structure [13, 36, 86, 89]. The mechanism discussed here is one possible route to adaptivity in natural neural networks. It can serve as the basis for more biologically detailed models [14, 15, 51].

Further applications of the network adaptation models are conceivable, e.g. to socio-economic systems. Network adaptation could in principle occur in adapting social links or economic ties of humans acting as agents in complex social or economic systems.

## References

1. Abraham, W.C., Mason-Parker, S.E., Bear, M.F., Webb, S., Tate, W.P.: Heterosynaptic metaplasticity in the hippocampus in vivo: A bcm-like modifiable threshold for ltp. *Proc. Natl. Acad. Sci. USA* **98**, 10924–10929 (2001). DOI 10.1073/pnas.181342098
2. Abraham, W.C., Tate, W.P.: Metaplasticity: A new vista across the field of synaptic plasticity. *Prog. Neurobiol.* **52**, 303–323 (1997)
3. Albert, R., Barabasi, A.L.: Dynamics of complex systems: Scaling laws for the period of boolean networks. *Phys. Rev. Lett.* **84**, 5660–5663 (2000)
4. Andrecut, M.: Mean field dynamics of random boolean networks. *J. Stat. Mech.* (2005). DOI 10.1088/1742-5468/2005/02/P02003
5. Anirvan M. Sengupta, M.D., Shraiman, B.: Specificity and robustness in transcription control networks. *Proc. Natl. Acad. Sci.* **99**, 2072–2077 (2002)
6. Bak, P.: *How Nature Works: The Science of Self-organized Criticality*. Copernicus, New York (1996)
7. Bak, P., Sneppen, K.: Punctuated equilibrium and criticality in a simple model of evolution. *Phys. Rev. Lett.* **71**, 4083–4086 (1993) DOI 10.1103/PhysRevLett.71.4083
8. Bak, P., Tang, C., Wiesenfeld, K.: Self-organized criticality: An explanation of the  $1/f$  noise. *Phys. Rev. Lett.* **59**, 381–384 (1987)
9. Barkai, N., Leibler, S.: Robustness in simple biochemical networks. *Nature* **387**, 913–916 (1997)
10. Bastolla, U., Parisi, G.: Closing probabilities in the kauffman model: An annealed computation. *Physica D* **98**, 1–25 (1996)
11. Bastolla, U., Parisi, G.: Relevant elements, magnetization and dynamical properties in kauffman networks: A numerical study. *Physica D* **115**, 203–218 (1998)
12. Bastolla, U., Parisi, G.: The modular structure of kauffman networks. *Physica D* **115**, 219–233 (1998a)
13. Beggs, J.M., Plenz, D. Neuronal avalanches in neocortical circuits. *J. Neurosci.* **23** 11167 (2003)
14. Beggs, J.M.: The criticality hypothesis: how local cortical networks might optimize information processing. *Phil. Trans. Roy. Soc. A* **366**(1864), 329–343 (2008). DOI 10.1098/rsta.2007.2092
15. Bertschinger, N., Natschläger, T., Legenstein, R.A.: At the edge of chaos: Real-time computations and self-organized criticality in recurrent neural networks. In: L.K. Saul, Y. Weiss, L. Bottou (eds.) *Advances in Neural Information Processing Systems* 17, pp. 145–152. MIT Press, Cambridge, MA (2005)

16. Bhattacharjya, A., Liang, S.: Median attractor and transients in random boolean nets. *Physica D* **95**, 29–34 (1996)
17. Bhattacharjya, A., Liang, S.: Power-law distributions in some random boolean networks. *Phys. Rev. Lett.* **77**, 1644–1647 (1996)
18. Bornholdt, S., Röhl, T.: Self-organized critical neural networks. *Phys. Rev. E* **67**, 066 118 (2003). DOI 10.1103/PhysRevE.67.066118
19. Bornholdt, S., Rohlf, T.: Topological evolution of dynamical networks: Global criticality from local dynamics. *Phys. Rev. Lett.* **84**, 6114–6117 (2000)
20. Bornholdt, S., Sneppen, K.: Neutral mutations and punctuated equilibrium in evolving genetic networks. *Phys. Rev. Lett.* **81**, 236–239 (1998)
21. Bornholdt, S., Sneppen, K.: Robustness as an evolutionary principle. *Proc. R. Soc. Lond. B* **267**, 2281–2286 (2000)
22. Christensen, K., Donangelo, R., Koiller, B., Sneppen, K.: Evolution of random networks. *Phys. Rev. Lett.* **81**, 2380 (1998)
23. Correale, L., Leone, M., Pagnani, A., Weigt, M., Zecchina, R.: The computational core and fixed point organization in boolean networks. *J. Stat. Mech.* (2006). DOI 10.1088/1742-5468/2006/03/P03002
24. Correale, L., Leone, M., Pagnani, A., Weigt, M., Zecchina, R.: Core percolation and onset of complexity in boolean networks. *Phys. Rev. Lett.* **96**, 018 101 (2006). DOI 10.1103/PhysRevLett.96.018101
25. Davidson, E.: *Genomic Regulatory Systems. Development and Evolution.* Academic Press, San Diego, CA (2001)
26. Derrida, B.: Dynamical phase transition in non-symmetric spin glasses. *J. Phys. A* **20**, 721–725 (1987)
27. Derrida, B., Flyvbjerg, H.: Distribution of local magnetisations in random networks of automata. *J. Phys. A* **20**, 1107–1112 (1987)
28. Derrida, B., Gardner, E., Zippelius, A.: An exactly solvable asymmetric neural network model. *Europhys. Lett.* **4**, 167 (1987)
29. Derrida, B., Pomeau, Y.: Random networks of automata: a simple annealed approximation. *Europhys. Lett.* **1**, 45–49 (1986)
30. Derrida, B., Stauffer, D.: Phase transitions in two-dimensional kauffman cellular automata. *Europhys. Lett.* **2**, 739ff (1986)
31. Drossel, B.: Extinction events and species lifetimes in a simple ecological model. *Phys. Rev. Lett.* **81**, 5011 (1998)
32. Drossel, B.: Number of attractors in random boolean networks. *Phys. Rev. E* **72**(1, Part 2) (2005). DOI 10.1103/PhysRevE.72.016110
33. Engert, F., Bonhoeffer, T.: Dendritic spine changes associated with hippocampal long-term synaptic plasticity. *Nature* **399**, 66–69 (1999)
34. Erdős, P., Rényi, A.: On the evolution of random graphs. *Publ. Math. Inst. Hung. Acad. Sci.* **5**, 17–61 (1960)
35. Flyvbjerg, H.: An order parameter for networks of automata. *J. Phys. A* **21**, L955–L960 (1988)
36. Gireesh, E.D., Plenz, D.: Neuronal avalanches organize as nested theta- and beta/gamma-oscillations during development of cortical layer 2/3. *Proc. Natl. Acad. Sci. USA* **105**, 7576–7581 (2008).
37. Gross, T., Blasius, B.: Adaptive coevolutionary networks: a review. *J. Roy. Soc. Interface* **5**, 259–271 (2008). DOI 10.1098/rsif.2007.1229
38. Hebb, D.O.: *The Organization of Behavior.* Wiley, New York (1949)
39. Kauffman, S.: Metabolic stability and epigenesis in randomly constructed genetic nets. *J. Theor. Biol.* **22**, 437–467 (1969)
40. Kauffman, S.: *The Origins of Order: Self-Organization and Selection in Evolution.* Oxford University Press, Oxford (1993)
41. Kaufman, V., Drossel, B.: Relevant components in critical random boolean networks. *New J. Phys.* **8** (2006). DOI 10.1088/1367-2630/8/10/228



42. Kaufman, V., Mihaljev, T., Drossel, B.: Scaling in critical random boolean networks. *Phys. Rev. E* **72**, 046 124 (2005). DOI 10.1103/PhysRevE.72.046124
43. Kelso, J.A.S., Bressler, S.L., Buchanan, S., DeGuzman, G.C., Ding, M., et al.: A phase transition in human brain and behavior. *Phys. Lett. A* **169**, 134–144 (1992)
44. Kesseli, J., Ramo, P., Yli-Harja, O.: Iterated maps for annealed boolean networks. *Phys. Rev. E* **74**(4, Part 2), 046 104 (2006). DOI 10.1103/PhysRevE.74.046104
45. Klemm, K., Bornholdt, S.: Stable and unstable attractors in boolean networks. *Phys. Rev. E* **72**(5, Part 2) (2005). DOI 10.1103/PhysRevE.72.055101
46. Krawitz, P., Shmulevich, I.: Basin entropy in boolean network ensembles. *Phys. Rev. Lett.* **98**(15) (2007). DOI 10.1103/PhysRevLett.98.158701
47. Kree, R., Zippelius, A.: Continuous-time dynamics of asymmetrically diluted neural networks. *Phys. Rev. A* **36**(9), 4421–4427 (1987). DOI 10.1103/PhysRevA.36.4421
48. Kürten, K.: Critical phenomena in model neural networks. *Phys. Lett. A* **129**, 156–160 (1988)
49. Kürten, K.: Correspondence between neural threshold networks and kauffman boolean cellular automata. *J. Phys. A* **21**, L615–L619 (1988b)
50. Langton, C.: Life at the edge of chaos. In: *Artificial Life*, vol. II, pp. 255–276. Addison-Wesley, Boston, MA (1991)
51. Levina, A., Herrmann, J.M., Geisel, T. Dynamical synapses causing self-organized criticality in neural networks. *Nat. Phys.* **3** 857–860 (2007)
52. Linkenkaer-Hansen, K., Nikouline, V.V., Palva, J.M., Ilmoniemi, R.J.: Long-range temporal correlations and scaling behavior in human brain oscillations. *J. Neurosci.* **21**, 1370–1377 (2001)
53. Liu, M., Bassler, K.E.: Emergent criticality from coevolution in random boolean networks. *Phys. Rev. E* **74**, 041 910 (2006). DOI 10.1103/PhysRevE.74.041910
54. Luque, B., Ballesteros, F.J., Muro, E.M.: Self-organized critical random boolean networks. *Phys. Rev. E* **63**, 051 913 (2001). DOI 10.1103/PhysRevE.63.051913
55. Luque, B., Ferrera, A.: Measuring mutual information in random boolean networks. *Complex Syst.* **12**, 241–252 (2000)
56. Luque, B., Sole, R.: Lyapunov exponents in random boolean networks. *Physica A* **284**(1–4), 33–45 (2000)
57. Luque, B., Sole, R.V.: Phase transitions in random networks: simple analytic determination of critical points. *Phys. Rev. E* **55**, 257–260 (1996)
58. Luscombe, N.M., et al.: M.M.B.: Genomic analysis of regulatory network dynamics reveals large topological changes. *Nature* **431**, 308–312 (2004)
59. Lux, T., Marchesi, M.: Scaling and criticality in a stochastic multi-agent model of a financial market. *Nature* **397**, 498–500 (1999). DOI 10.1038/17290
60. Malamud, B.D., Morein, G., Turcotte, D.L.: Forest fires: An example of self-organized critical behavior. *Science* **281**, 1840–1842 (1998)
61. McGuire, P.C., Bohr, H., Clark, J.W., Haschke, R., Pershing, C.L., Rafelski, J.: Threshold disorder as a source of diverse and complex behavior in random nets. *Neural Networks* **15**, 1243–1258 (2002)
62. li Ming, G., Wong, S.T., Henley, J., bing Yuan, X., jun Song, H., Spitzer, N.C., Poo, M.m.: Adaptation in the chemotactic guidance of nerve growth cones. *Nature* **417**, 411–418 (2002)
63. Molgedey, L., Schuchard, J., Schuster, H.G.: Suppressing chaos in neural networks by noise. *Phys. Rev. Lett.* **69**, 3717 (1992)
64. Murray, J.: *Mathematical Biology*. Springer, New York (2002)
65. Nakamura, I.: Dynamics of threshold network on non-trivial distribution degree. *Eur. Phys. J. B* **40**, 217–221 (2004). DOI 10.1140/epjb/e2004-00260-4
66. Nicolis, G., Prigogine, I.: *Self-Organization in Nonequilibrium Systems: From Dissipative Structures to Order Through Fluctuations*. Wiley, New York (1977)
67. Nykter, M., Price, N.D., Aldana, M., Ramsey, S.A., Kauffman, S.A., Hood, L.E., Yli-Harja, O., Shmulevich, I.: Gene expression dynamics in the macrophage exhibit criticality. *Proc. Natl. Acad. Sci. USA* **105**(6), 1897–1900 (2008). DOI 10.1073/pnas.0711525105

68. Nykter, M., Price, N.D., Larjo, A., Aho, T., Kauffman, S.A., Yli-Harja, O., Shmulevich, I.: Critical networks exhibit maximal information diversity in structure-dynamics relationships. *Phys. Rev. Lett.* **1**(5) (2008). DOI 10.1103/PhysRevLett.100.058702
69. van Ooyen, A.: Competition in the development of nerve connections: a review of models. *Network: Computation in Neural Systems* **12**, R1–R47 (2001)
70. Paczuski, M., Bassler, K.E., Corral, A.: Self-organized networks of competing boolean agents. *Phys. Rev. Lett.* **84**, 3185–3188 (2000). DOI 10.1103/PhysRevLett.84.3185
71. Paczuski, M., Maslov, S., Bak, P.: Avalance dynamics in evolution, growth and depinning models. *Phys. Rev. E* **53**, 414–443 (1996)
72. Rämö, P., Kesseli, J., Yli-Harja, O.: Perturbation avalanches and criticality in gene regulatory networks. *J. Theor. Biol.* **242**, 164–170 (2006). DOI 10.1016/j.jtbi.2006.02.011
73. Ribeiro, A.S., Kauffman, S.A., Lloyd-Price, J., Samuelsson, B., Socolar, J.E.S.: Mutual information in random boolean models of regulatory networks. *Phys. Rev. E* **77**(1, Part 1) (2008). DOI 10.1103/PhysRevE.77.011901
74. Rohlf, T.: Networks and Self-Organized Criticality. Master's thesis, Christian-Albrechts-Universität Kiel (Germany) (2000)
75. Rohlf, T.: Critical line in random threshold networks with inhomogeneous thresholds. *Phys. Rev. E* **78**, 066118 (2008)
76. Rohlf, T.: Self-organization of heterogeneous topology and symmetry breaking in networks with adaptive thresholds and rewiring. *Europhys. Lett.* **84**, 10004 (2008)
77. Rohlf, T., Bornholdt, S.: Criticality in random threshold networks: Annealed approximation and beyond. *Physica A* **310**, 245–259 (2002)
78. Rohlf, T., Bornholdt, S.: Gene regulatory networks: A discrete model of dynamics and topological evolution. In: A. Deutsch, J. Howard, M. Falcke, W. Zimmermann (eds.) *Function and Regulation of Cellular Systems: Experiments and Models*. Birkhäuser Basel (2004)
79. Rohlf, T., Gulbahce, N., Teuscher, C.: Damage spreading and criticality in finite dynamical networks. *Phys. Rev. Lett.* **99**, 248701 (2007). DOI 10.1103/PhysRevLett.99.248701
80. Schmoltzi, K., Schuster, H.G.: Introducing a real time scale into the Bak-Sneppen model. *Phys. Rev. E* **52**, 5273–5280 (1995).
81. Schroeder, B.C., Kubisch, C., Stein, V., Jentsch, T.: Moderate loss of function of cyclic-amp-modulated *kcng2/kcng3*  $K^+$  channels causes epilepsy. *Nature* **396**, 687–690 (1998). DOI 10.1038/25367
82. Shmulevich, I., Kauffman, S.A., Aldana, M.: Eukaryotic cells are dynamically ordered or critical but not chaotic. *Proc. Natl. Acad. Sci. USA* **102**, 13439–13444 (2005)
83. Sole, R., Luque, B.: Phase transitions and antichaos in generalized kauffman networks. *Phys. Lett. A* **196**, 331–334 (1995)
84. Sole, R.V., Manrubia, S.C.: Criticality and unpredictability in macroevolution. *Phys. Rev. E* **55**, 4500–4507 (1997)
85. Sornette, D.: Critical phase transitions made self-organized: a dynamical system feedback mechanism for self-organized criticality. *J. Phys. I France* **2**, 2065–2073 (1992)
86. Stewart, C.V., Plenz, D. Homeostasis of neuronal avalanches during postnatal cortex development in vitro. *J. Neurosci.* **169**, 405–416 (2008)
87. Teuscher, C., Sanchez, E.: Self-organizing topology evolution of turing neural networks. *Artificial Neural Networks - ICANN 2001, Proceedings* **2130**, 820–826 (2001)
88. Thomas, R.: Boolean formalization of genetic control circuits. *J. Theor. Biol.* **42**, 563–585 (1973)
89. Trachtenberg, J.T., Chen, B.E., Knott, G.W., Feng, G., Sanes, J.R., Walker, E., Svoboda, K.: Long-term in vivo imaging of experience-dependent synaptic plasticity in adult cortex. *Nature* **420**, 788–794 (2002)
90. Wagner, A.: Robustness against mutations in genetic networks of yeast. *Nat. Genet.* **24**, 355–361 (2000)
91. Wooters, W.K., Langton, C.G.: Is there a sharp phase transition for deterministic cellular automata? *Physica D* **45**, 95–104 (1990)